Bull Volcanol (2007) 69: 365–372
DOI 10.1007/s00445-006-0081-6

RESEARCH ARTICLE

Raffaello Trigila · Maurizio Battaglia · Michael Manga

An experimental facility for investigating hydromagmatic eruptions at high-pressure and high-temperature with application to the importance of magma porosity for magma-water interaction

Received: 16 September 2003 / Accepted: 16 March 2006 / Published online: 28 June 2006

Abstract An experimental facility has been developed to investigate magma-water interaction (MWI). The facility operates in a high-pressure and high-temperature environment, with temperatures up to 1,200°C and pressures up to 200 MPa. Cylindrical sample-holders (20 by 180 mm in size) are heated conductively to yield a three phase (melt, crystals and gas) system, and then water (or other fluid) is injected into the sample through a capillary tube (diameter 0.5 mm, length ca. 1,000 mm) under controlled conditions. Pressure, volume and temperature changes are continuously recorded during every phase of the experiments. To test this facility, MWI is studied at subliquidus temperatures (800 and 900°C) and pressure (8 MPa), using a leucite tephrite sample with two different initial grain sizes. Because of the grain-size dependence of sintering, the two starting materials produce magmas with different textures at the same temperature: porous magma for large initial grain sizes and dense magma for small initial grain sizes. In these experiments 1.5 g of water at room temperature is injected into 6.0 g of partially molten sample at velocities ranging from 1 to 3 m/s. We find that the extent of fragmentation and transport caused by MWI are mainly controlled by the texture of the interacting sample with explosive interaction occurring only for porous magmas.

Keywords Experimental volcanology · Hydro-magmatism · Magma-water interaction · Volcanic MFCI · HPHT facility · Latera volcano · Spatter flow

Editorial responsibility: D. Dingwell

R. Trigila (✉)
Dipartimento di Scienze della Terra, Universita' degli Studi di Roma "La Sapienza",
P.le A Moro 5,
00185 Roma, Italy
e-mail: raffaello.trigila@uniroma1.it
Tel.: +39-06-4456634
Fax: +39-06-49914926

M. Battaglia · M. Manga
Department of Earth and Planetary Science,
UC Berkeley,
307 McCone Hall,
Berkeley, CA 94720, USA

M. Battaglia
Department of Structural Geology and Geodynamics,
University of Goettingen,
Goldschmidtstr. 3,
37077 Goettingen, Germany

Introduction

Explosive eruptions resulting from the conversion of groundwater into steam by direct contact with ascending magma (the so-called phreatomagmatic eruptions) can range from single, small events to prolonged, devastating eruptions (White and Houghton 2000; Houghton et al. 2000; Palladino et al. 2001). Several well-known historical eruptions show evidence of interaction of magma with water in soil or rocks, or pouring of water into volcanic conduits and magma reservoirs (see Dobran and Papale 1993 and references therein). When magma and water come into contact, a vapor film is created at the magma/water interface. If the film becomes unstable and collapses, the water will directly contact the magma and blast into steam, generating an explosive hydromagmatic eruption (Francis 1993, p. 128).

A number of theoretical investigations on explosive magma-water interaction (MWI) have been recently performed (Dobran and Papale 1993; Koyaguchi and Woods 1996; Dobran 2002; Raue 2004). Nevertheless, theoretical modeling of magma-water interaction remains difficult because of the poorly understood initial and boundary conditions and triggering mechanisms that lead to efficient magma-water mixing (Dobran 2002, p. 442). For this reason, laboratory investigations play a major role in understanding the physics of explosive MWI (see Zimanowski 1998, and references therein; Büttner and Zimanowski 1998; Büttner et al. 2002; Zimanowski and Büttner 2002).

Explosive MWI has been extensively studied using the theoretical and experimental framework of volcanic molten fuel coolant interaction (MFCI) (Sheridan and Wohletz 1983; Wohletz 1986; Zimanowski et al. 1991; Wohletz and

Heiken 1992; White 1996; Büttner and Zimanowski 1998; Büttner et al. 2002). In the earliest experiments (e.g., Wohletz 1986), emphasis was given to studying the explosive interaction between a molten fuel (e.g., thermite) and a coolant (water). Later experiments (e.g., Zimanowski et al. 1997; Büttner and Zimanowski 1998; Büttner et al. 2002) were specifically designed to record the short term dynamics of a volcanic MFCI, and employed re-melted volcanic rocks as molten fuel. In their typical experimental run, several hundred grams of granulated volcanic material were placed in a steel crucible and inductively heated to create about 100 ml of melt under atmospheric conditions. Water was injected into the melt and the explosion was externally triggered by shooting a projectile (air gun bullet) onto the melt surface. A number of transducers recorded force and pressure history during the experiments. Furthermore, high-speed cinematography was used to measure the expansion velocities and to distinguish the various volcanic MFCI phases from each other (e.g., Büttner et al. 2002).

A volcanic MFCI has four essential stages (Zimanovski et al. 1997): (1) mixing of water and melt under stable film boiling conditions, controlled by density and viscosity differences between water and melt; (2) vapor film collapse leading to direct contact between melt and water; (3) fine fragmentation and rapid increase of heat transfer, which results in positive feedback; and (4) system expansion and generation of superheated steam.

Several physical models have been proposed to explain the high conversion ratio from thermal to kinetic energy deduced from experiments and volcanic eruptions. Studies on basaltic eruptions that produced widespread tephra at Kilauea volcano (Hawaii) suggest that the erupting magma was turbulent and would have mixed with surrounding water in vortices ranging downward in size to centimeters (Mastin et al. 2004). Such fine-scale mixing would have ensured rapid heat exchange and extensive magma fragmentation, maximizing the violence of these eruptions. In the case of high viscosity, low superheated melts, the generation of such homogeneous (fine scale) mixing is unlikely (e.g., Zimanowski and Büttner 2002). Büttner and Zimanowski (1998), presented experimental results identifying the major contributor of explosion energy as thermo-hydraulically induced brittle fragmentation of the melt and heat transfer during stage 3 of MFCI. It is worth noting that there is geological evidence that volcanic MFCI may involve mixing of magma with impure sediment-laden water, further complicating efforts of reconstructing explosive MWI in a laboratory (White 1996).

Here, we describe in detail a new experimental facility specifically designed to investigate MWI under pressure and temperature conditions corresponding to those existing during volcanic eruptions (e.g., Trigila 2004). The findings presented in this paper are obtained by performing experiments at low pressure (8 MPa) and sub-liquidus temperature (800 and 900°C) in an entrapment configuration. Test samples (partially remelted volcanic rock into which we inject water at room temperature) are prepared under well-constrained boundary conditions (confining pressure, melt temperature, magma-water ratio), in a half-ton IHPV (internally heated pressure vessel). Magma-water mixing (stage 1 of volcanic MFCI) and vapor film collapse (stage 2), prerequisites to induce the steam explosion (stage 3 and 4), are not induced by any external triggering signal (e.g., Zimanowski et al. 1991; Shamoun and Corradini 1997). We use as starting material a leucite tephrite sample from a spatter-flow deposit in the Latera volcanic complex (Vulsini Volcanic District, Italy) that represents the transition of eruptive style from magmatic to hydromagmatic (Palladino and Taddeucci 2000). To simulate the effects of heterogeneities (see e.g., White 1996), we employ a starting granular material with coarse grain size. In our experiments we find that MWI is mainly controlled by the sample texture and grain size distribution of the interacting material.

Experimental facility

The magma-water interaction experiments were conducted at the HPHT (high pressure/high temperature) Laboratory of the University of Rome "La Sapienza". The experimental facility (Fig. 1) consists of four units: (1) the interaction unit, (2) the water injection unit, (3) the pressure, volume and temperature (PVT) control and recording unit, and (4) the gas compression unit.

The facility is designed to operate at high pressures and high temperatures under well-constrained boundary conditions. These experiments are performed in an entrapment configuration, where water is dispersed in the partially molten material. Test melts are prepared under specified pressure and temperature conditions in cylindrical sample-holders (20 by 180 mm in size). Water is then injected into the melt. It is worth noting that this facility allows investigating the interaction between a volcanic melt and other fluids (e.g., CO_2) as well.

Pressure, volume and temperature (PVT) data are continuously recorded (Fig. 2) during the experiments by a computer-controlled data logger (PVT recording unit). The gas compression unit supplies the pressure vessel with gas Argon via a HASKEL booster able to reach pressures up to 250 MPa.

Interaction unit

Water-melt mixing and explosive interaction take place in the interaction unit (Fig. 3). The main component of this unit is a large volume (100 mm internal bore) pressure vessel, containing the interaction cell and the heating device, a two-zone KANTHAL A-1 furnace. The vessel operates up to pressures of 200 MPa and temperatures of 1,200°C. Pressure and temperature control and recording are regulated and controlled by two pressure transducers (WIKA 89X.13XXX–piezoresistive sensor elements type) that measure the pressure in the interaction cell and external chamber, and two Pt/Pt-13%Rh thermocouples that measure temperatures at the top and bottom of the sample holder.

The silicate melt sample holder is located in the inner part of the interaction cell. The sample-holder, an

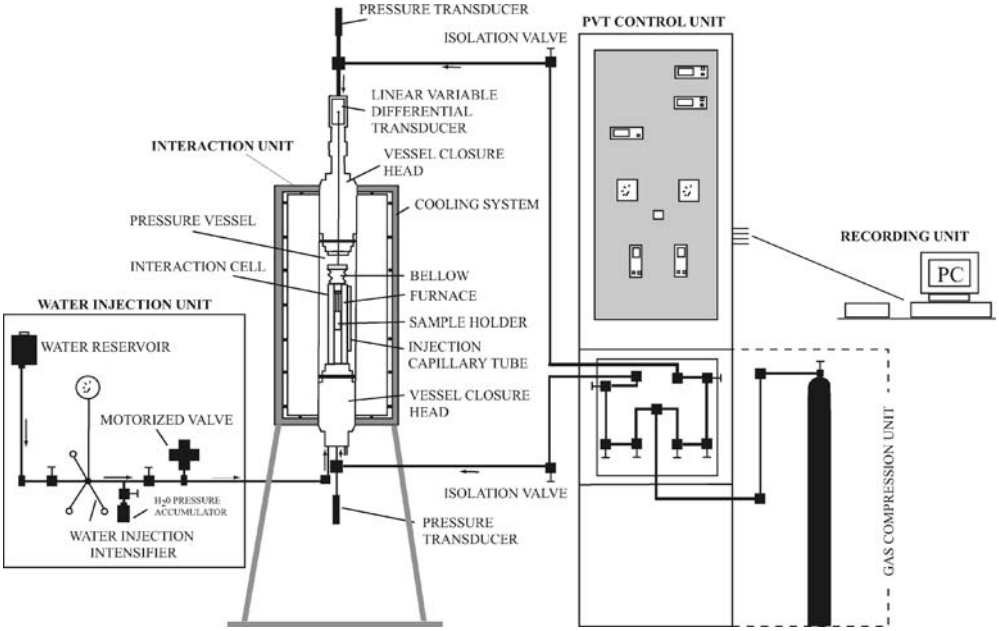

Fig. 1 View of the experimental facility. See text for explanation

INCONEL 600 super-alloy cylinder 20×180 mm in size, occupies the heated area of the interaction cell. If melt fragmentation and ejection occurs, the ejected fragments are collected into a gasket 20 mm in diameter, at the top of the sample holder (Fig. 3b).

The interaction cell is made up of a cylindrical stainless steel case containing a two-zone furnace controlled by two thermocouples. The cell has a gas argon inlet placed at the bottom while the top is closed by an INCONEL 600 bellows. The capillary enters the sample holder beneath the bellows. The sample is placed within a cylindrical cavity that is 16 mm in diameter (narrowing up to a 3 mm "conduit") and 100 mm long. A linear variable differential transducer (LVDT) on top of the bellows measures volume changes. We take into account the non-linear mechanical response of the bellows to the pressure rise by estimating an empirical bellows' damping coefficient (Fig. 4a).

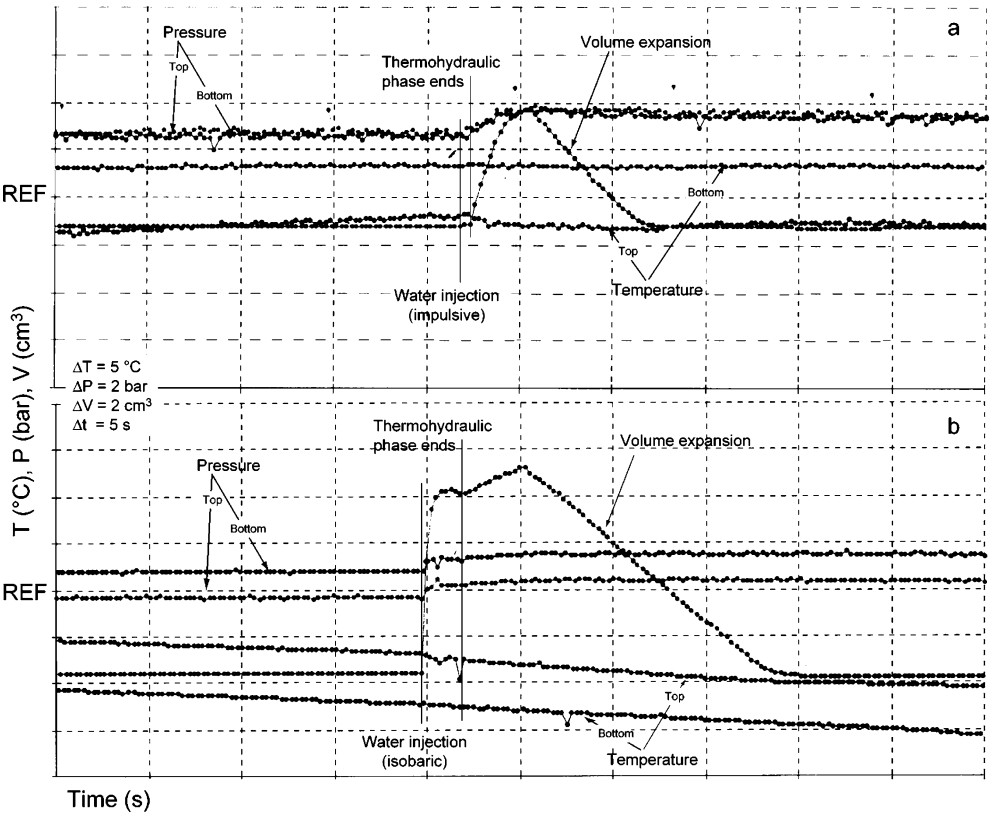

Fig. 2 Example records or pressure, volume and temperature as a function of time. Reference values for the figure: pressure 7.5 MPa (*top and bottom*); volume 210 cm^3; temperature 950°C (*bottom*) and 700°C (*top*). **a** Impulsive (constant injection mass) run; **b** isobaric (constant injection pressure) run

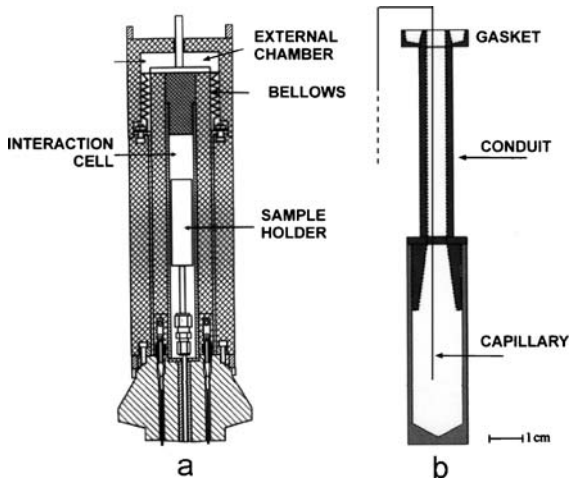

Fig. 3 **a** Cross-section of the interaction unit (not to scale); **b** cross-section of the interaction cell. See text for explanation

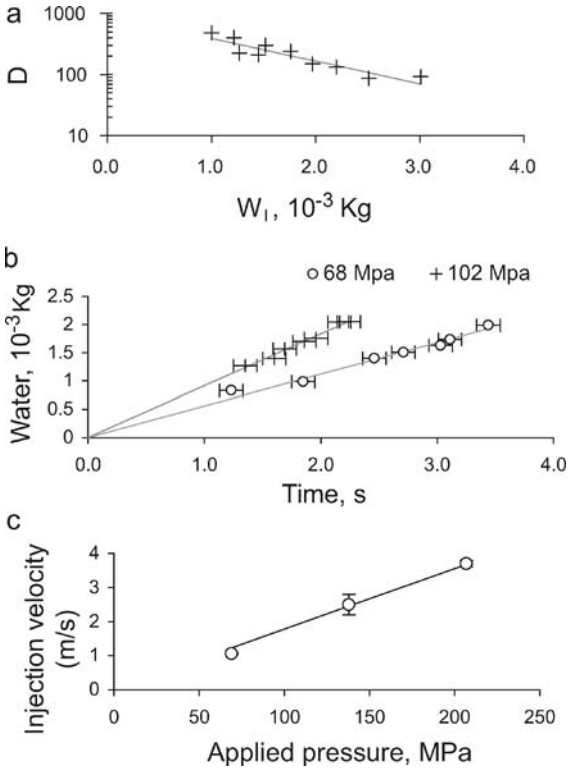

Fig. 4 Calibration of the experimental apparatus. **a** Bellows' damping coefficient D. To estimate D, we performed a number of calibration runs (T=800°C; P_C=8 MPa) injecting water on a solid ceramic cylinder. The calibration curve is $Log_{10}(D) = a \cdot m + b$, where a = −0.36±0.5 10^{-3} kg^{-1} and b=2.9±0.1. *Error bars* are negligible at the plot scale. **b** Calibration curves of mass of injected water vs. injection time for the constant injection pressure (isobaric) runs (capillary ∅=0.5 mm). Confining pressure P_C=8 MPa. Slopes: (0.56±0.01)×10^{-3} kg/s (68 MPa curve); (0.92±0.01)×10^{-3} kg/s (102 MPa curve). **c** Injection velocity as a function of the injection pressure (capillary ∅=0.8 mm)

Water injection unit

The water injection unit is equipped with a motorized valve that allows the injection of precise volumes of water into the silicate melt sample. The injected water has a separate pressurization system (water injection intensifier) working up to 700 MPa, and enters the sample holder at room temperature via a capillary tube (0.5 mm in diameter; Fig. 3b). A valve-assisted circuit can connect or isolate the sample holder from the pressure vessel, leaving the same pressure across the bellows or creating a modest differential pressure between the outside and the inside of the interaction cell.

The amount of water injected into the melt is controlled through the injection pressure and time. Calibration curves of mass of injected water versus injection time were computed at constant ("isobaric" test; Fig. 4b) and decaying ("impulsive" test) pressure. Isobaric calibration curves were determined by injecting water at a constant pressure of 68 MPa (or 102 MPa) into the capillary. We used a high-speed digital camera to measure the water injection velocity (Fig. 4c). To estimate the mass of water injected during the isobaric injection experiments, the injection pressure was kept constant through the injection period by connecting the injection circuit with a 2-L high-pressure reservoir. The injection period was then measured with a chronometer (precision 0.1 s); the injected water ejected from the capillary over several injections periods was finally collected and weighted using an analytical balance. The mass of the injected water for the "impulsive" tests was determined by weighting the water directly discharged from the intensifier after calibration at several pressures between 34 and 306 MPa.

Experiments and experimental materials

Chemical and modal analysis of the leucite-tephrite sample used in our experiments is given in Table 1. In each experimental run (Table 2), the sample holder is filled with finely powdered (grain diameter below 10 μm) or granulated (grain diameter 0.7 mm) volcanic rock and heated conductively (heating gradient: 600°C/h) to the experiment temperature. The sample is left at the experiment temperature for 30 min, then water at room temperature is injected into the sample at a velocity between 1 and 3 m/s (Fig. 4c) through the capillary (Fig. 3b). The water-magma ratio is close to what is considered the optimal 0.3 value (White 1996). We let the system evolve without any external influence: the vapor film collapse (stage 2 of a MFCI) is not induced by an external trigger (e.g., Büttner et al. 2002) but is controlled by the characteristics of the sample-water mixing, i.e., any eruption is self-triggered.

The use of two different grain sizes for the starting materials insures a different texture (in particular, porosity) of the magma that interacts with water. The sintering or densification of the starting material is driven by the surface free energy of the particles and consequently depends of the size (e.g., Frenkel 1945; Mackenzie and Shuttleworth 1949) and size-distribution (e.g., Prado et al. 2001) of particles. For the temperatures and run times of the experiments reported here, sintering is complete for the samples that begin as powders (Fig. 5a). For the granular

Table 1 Chemical and modal analysis of the sample used in the MWI experiments

Chemical analysis		Modal analysis (vol.%)	
SiO_2	49.14	Welded ash groundmass	57.4
TiO_2	0.80	Light pumices	16.4
Al2O3	18.58	Dark pumices	12.2
Fe_2O_3	3.78	Igneous xenoliths	7.9
FeO	2.99	Sed+Met. xenoliths	3.1
MnO	0.10	Leucite+sanidine	0.1
MgO	3.14	Plagioclase	0.8
CaO	8.36	Biotite	0.1
Na_2O	3.11	Pyroxene	1.9
K_2O	6.73	Opaques	0.1
P_2O_5	0.76		
Cl-	0.05		
BaO	0.18		
LOI	2.38		

starting materials, the sample retains most of its porosity and forms a fragile aggregate (Fig. 5b). We verified these textural differences in experiments in which water was not injected (Fig. 5). The difference in texture of the magma that interacts with water is the key for the results presented here, and the use of different starting grain sizes allows us to study MWI for samples with identical thermal energies in which the only difference is magma porosity.

Results and discussion

In our experiments, although performed with a basic alkaline composition, the viscosity contrast between melt and water is sufficiently large that it should inhibit their hydrodynamic mixing (e.g., Sundararaj and Macosko 1995; Zimanowski et al. 2004). Instead, the results listed in Table 2 and shown in Fig. 6 indicate that thermo-hydraulic explosive interactions occur only for the experiments with the granular starting material. We thus conclude that the residual porosity of the solid grains-melt mixture plays an essential role in MFCI, probably by allowing rapid flow of water into the porous magma, a process that is equivalent to hydrodynamic mixing in nonporous magmas. About 0.1 s after the injection, the reacting water reaches a critical state and transforms into superheated steam. Once the steam forms, the thermohydraulic phase is terminated and the system expands to the confining pressure P_C (Fig. 2).

We use two different parameters to describe quantitatively the MWI: (1) the percentage of the mass ejected and collected into the gasket, and (2) the mechanical efficiency E of the explosion (Wohletz 1986). E is determined by the portion of the trapped rapidly vaporizing coolant (water) inducing fragmentation of the molten fuel. Using estimates of the work W and potential energy ΔE_P, we can compute a lower bound for E as follows:

$$E \geq \frac{\Delta E_P}{W} = \frac{Mgh}{P_c V_B} \quad (1)$$

where g is the gravity acceleration and h the height between the sample holder and the gasket. The work W is proportional to the bellows' volume change V_B, and the system confining pressure P_C. V_B increases because the pressure increases in the interaction unit as water vaporizes. To avoid the possibility of the bellows breaking during the experiments or measuring only saturation

Table 2 MWI experiments

Run #	Sample[a]	Water injection mode	T (°C)	Water-melt mass ratio	$V_B \pm \Delta V_B$ (10^{-9} m^3)	Transported mass (wt %)	Particle size analysis	
							Left–sample holder Modal class (μm)	Transported–gasket- Modal class (μm)
41	Granular	Impulsive	800	0.36	450±23	16.5	1,230	1,230
51	Granular	Impulsive	800	0.34	793±40	25.4	1,030	1,030
45	Granular	Isobaric	800	0.33	277±14	23.5	1,030	1,030
42	Granular	Impulsive	900	0.34	796±40	29.6	1,030	1,030
47	Granular	Isobaric	900	0.35	307±15	12.5	1,030	1,030
49	Powder	Impulsive	800	0.34	477±24	0.0	610	N/A
43	Powder	Impulsive	800	0.34	403±20	0.3	75	75
46	Powder	Isobaric	800	0.40	180±9	0.0	180	N/A
48	Powder	Isobaric	900	0.34	161±8	1.2	180	N/A
44	Powder	Impulsive	900	0.34	451±23	1.2	75	75
Confining pressure P_C=8.0 MPa; water injection pressure P_I=102 MPa; reservoir volume V_R=(19±1)×10^{-6} m^3								
Melt material properties[b]	800°C		Viscosity: 5.6×10^4 Pas		Density: 2,360 kg/m^3		Specific heat: 1,493 J/kg K	
	900°C		Viscosity: 7.7×10^3 Pas		Density: 2,340 kg/m^3		Specific heat: 1491 J/kg K	

[a]The two samples have a homogenous initial grain size distribution (700 μm for the granular sample and 5 μm for the powder sample)
[b](Ghiorso et al. 1994)

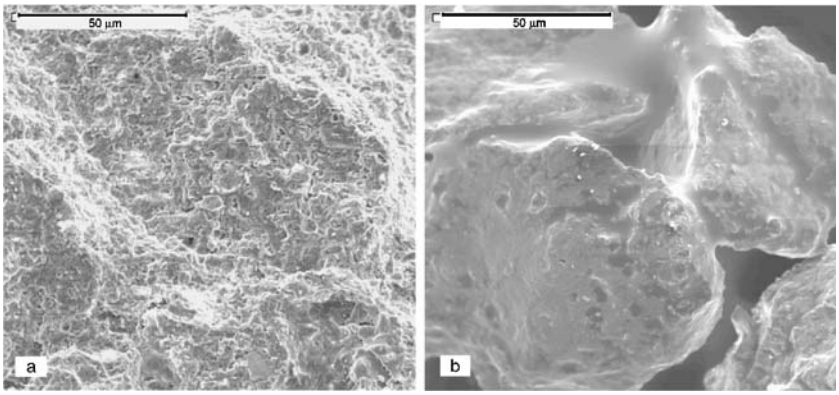

Fig. 5 Scanning electron microscope images of starting material at sub-liquidus temperature, no water injected. **a** Powdered starting material. Note the homogeneous melt distribution; **b** Granular starting material. Melt is present at the contact between grains, creating a fragile porous aggregate

values for W, the argon line above the bellows is connected to a large volume reservoir (volume V_R=18.8 cm^3). Also we take into account the non-linear mechanical response of the bellows to the pressure increase by estimating an empirical damping coefficient D (Fig. 4a)

$$V_B = \frac{mv - V_R}{D} \quad (2)$$

where m is the mass of injected water, and v is the specific volume of water.

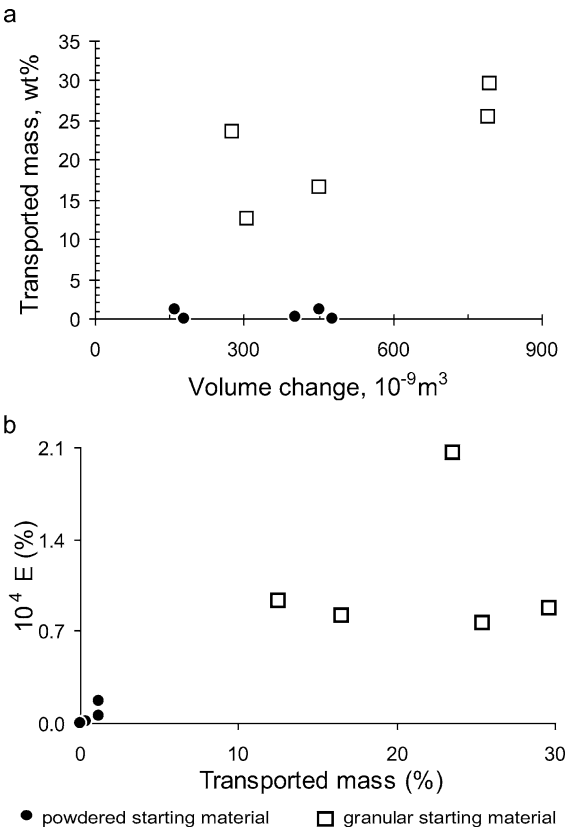

Fig. 6 Experimental results. **a** Transported mass (wt% is the weight % of the initial mass). Experimental runs with smaller grain size samples (powdered starting material) show little or no mass transport. **b** Efficiency E (see Eq. 1). The greatest conversion rate of thermal energy into mechanical energy is measured in the experiments with granular samples

Figure 6 shows that negligible or no mass transport is achieved in experiments employing powdered starting material, (grain size below 10 µm). This observation is in agreement with the low efficiency E computed for the same experiments. Both observations are important (but not sufficient) indicators that explosive MWI has been achieved only in runs with granular samples (grain size 0.7 mm). The scanning electron microscope image reported in Fig. 7 shows an example of some the features created in experiments with the powdered starting material. While the sample has cracked because of the rapid cooling induced by water injection, there is no evidence of features indicative of explosive magma-water interaction.

The results of grain size analyses performed with a Sympathec Helos particle size analyzer are shown in Fig. 8. The grain size histograms come from experiments with different initial and boundary conditions: impulsive (Fig. 8a) or isobaric (Fig. 8b) water injection, different temperatures, and texture of starting material. The histograms show different sizes in the transported fragments according to the type of starting material. In the case of granular starting material, ejected fragments have a

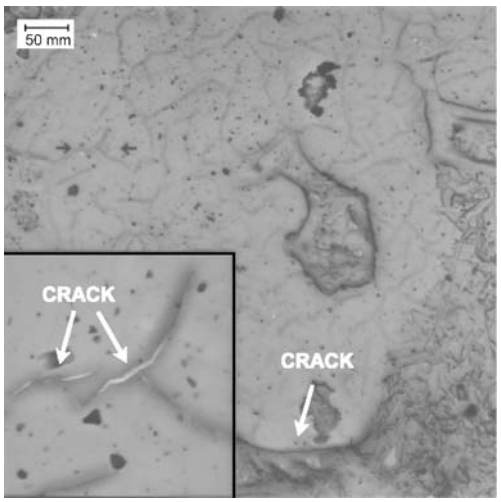

Fig. 7 The scanning electron-microscope thin-section image shows an example of some of the features created in experiments at subliquidus temperature (900°C) with the powdered starting material. Note the cracks induced by cooling when water is injected into the sample at constant pressure (102 MPa). The image shows no evidence of explosive MWI

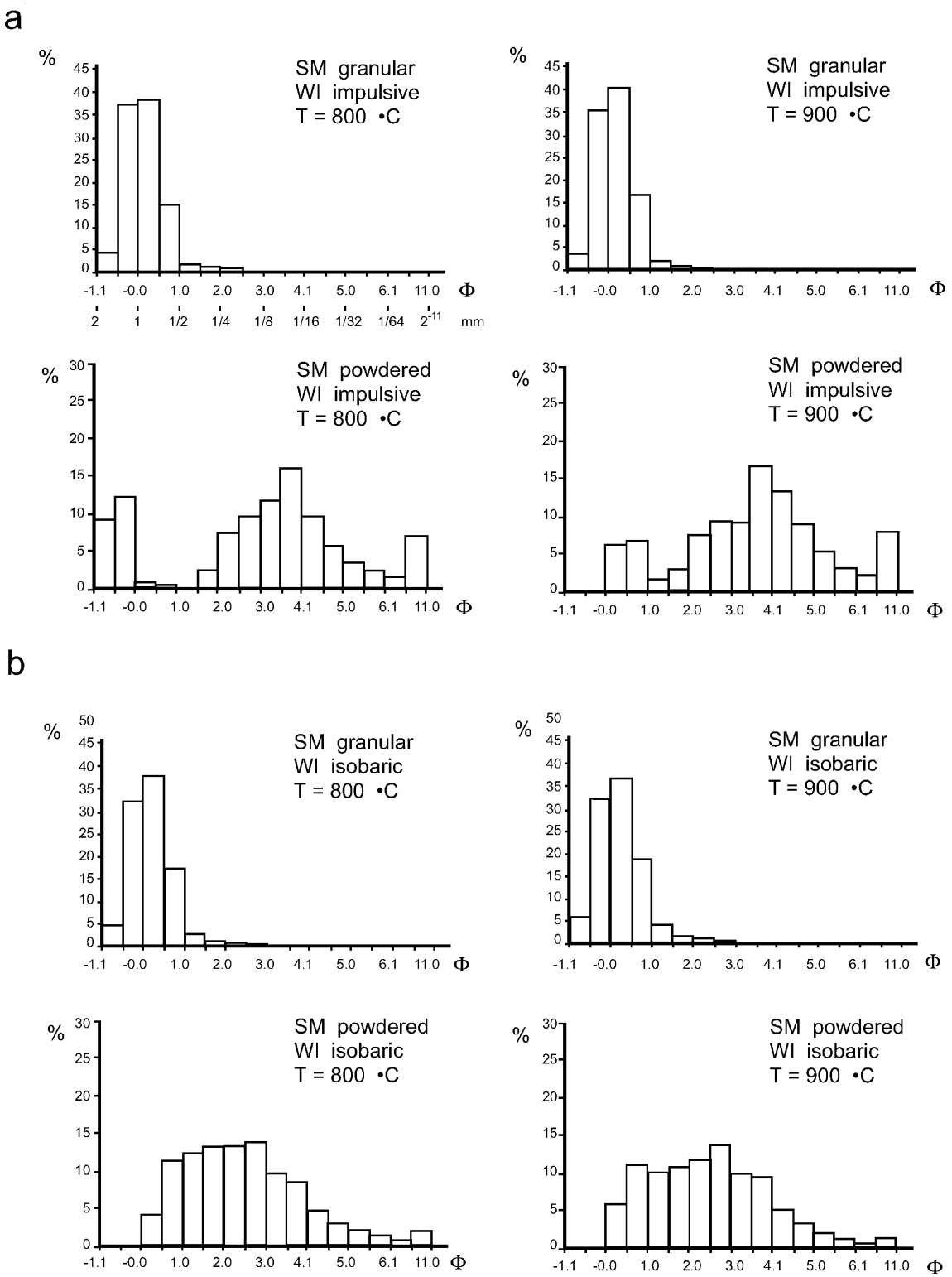

Fig. 8 Grain size distribution of ejected particles collected in the gasket. The original size distribution is homogeneous both for the powder (Φ=10 μm) and granular sample (Φ=0.7 mm). The multimodal distribution of the powdered starting material (SM)—with maximums around 1 mm and 1/8 mm—indicates that fine grains melted together to form larger particles. The grain size distribution of the granular starting material does not really change. This means that the explosive MWI separated particles glued together by a thin film of melt

unimodal distribution close to the size of the original particles, while the finely powdered starting material results in broad distribution between few microns and few hundreds of microns. It appears that, in the first case, the fragmentation operates on the thin melt interface between the solid grains, while in the second case the

multimodal distribution indicates different interfacial accelerations throughout sample volume.

Summary

A set of laboratory experiments on MWI has been performed using an instrumental facility capable of operating at high pressure and high temperature under well-constrained conditions. This facility allows several variables to be controlled including: mass, pressure, and modes of water injection, and the mass and pressure of the starting material. In each experiment, it is possible to monitor the volume expansion, temperature and pressure variations due to the interaction (Fig. 2) and collect and analyze the sample fragments ejected in the course of the interaction itself. Given the large number of variables, the experiments reported here can be viewed as exploratory.

In this study, we considered only the role of magma porosity on the magma–water interaction for a magma containing solid, melt and gas components. The fragmentation process and transport are controlled by the nature of the interacting sample. If the interacting sample is porous, in our case made of large solid grains (0.7 mm average diameter) welded by interstitial melt (Fig. 5b), the transported fragments can represent up to 30% of the original weight and have a grain size that corresponds to the original one of the starting material (Fig. 8). If the interacting sample is made of melt including microlites (10 μm average diameter), transport is around 1% and the collected fragments range in grain size from few microns to few hundreds of microns (Fig. 8). We thus conclude that different eruption styles would result from different porosities of the magma, and, according to the experimental evidence, the porous samples can erupt explosively giving a significant transport. We suggest that the mixing stage of MFCI occurs, in this case, as water "mixes" by porous flow with the hot magma.

Acknowledgements This research was financed by the Gruppo Nazionale di Vulcanologia–Framework Program 2000–2004, as part of Project 09: Eruptive scenarios from Physical Modeling and Experimental Volcanology. Maurizio Battaglia and Michael Manga were supported by the NSF grant EAR 0207471. Many thanks to Prof. B. Landini who made the granulometric analyses possible.

References

Büttner R, Zimanowski B (1998) Physics of thermohydraulic explosions. Phys Rev E 57:5726–5729

Büttner R, Dellino P, La Volpe L (2002) Thermohydraulic explosions in phreatomagmatic eruptions as evidenced by the comparison between pyroclasts and products from molten fuel coolant interaction experiments. J Geophys Res 107 (B11):2277, DOI:10.1029/2001JB000511

Dobran F (2002) Volcanic processes: mechanisms in material transport. Kluwer, New York

Dobran F, Papale P (1993) Magma-water interaction in closed systems and application to lava tunnels and volcanic conduits. J Geophys Res 98:4231–4259

Francis P (1993) Volcanoes: planetary perspective. Clarendon, Oxford

Frenkel J (1945) Viscous flow of crystalline bodies under the action of surface tension. J Phys USSR 9:345

Ghiorso MS, Hirschmann MM, Sack RO (1994) New software models thermodynamics of magmatic systems. EOS 75:575–576

Houghton BF, Wilson CJN, Smith RT, Gilbert JS (2000) Phreatoplinian eruptions. In: Sigurdsson H et al (eds) Encyclopedia of volcanoes. Academic Press, San Diego pp 513–516

Koyaguchi T, Woods AW (1996) On the formation of eruption columns following explosive mixing of magma and surface-water. J Geophys Res 101:5561–5574

Mackenzie JK, Shuttleworth R (1949) A phenomenological theory of sintering. Proc R Soc London B 62:833

Mastin LG, Christiansen RL, Thornber C (2004) What makes hydromagmatic eruptions violent? Some insights from the Keanakako'i Ash, Kilauea Volcano, Hawai'i. J Volcanol Geotherm Res 137:15–31

Palladino DM, Taddeucci J (2000) Alternating Strombolian and hydromagmatic activities: a study case from the Latera Volcano (Vulsini, Italy). In: Abstracts of IAVCEI General Assembly 2000, Bali (Indonesia), 18–22 July 2000

Palladino DM, Gaeta M, Marra F (2001) A large K-foiditic hydromagmatic eruption from the early activity of the Alban Hills Volcanic District, Italy. Bull Volcanol 63:345–359

Prado MO, Zanotto ED, Zolkin VM (2001) Model for sintering of polydisperse glass particles. J Non-Cryst Solids 279:169–178

Raue H (2004) A new model for the fracture energy budget of phreatomagmatic explosions. J Volcanol Geotherm Res 129:99–108

Shamoun B, Corradini ML (1997) Supercritical vapor explosions: comparisons between thermodynamics and mechanistic models. Nucl Technol 120:158–170

Sheridan MF, Wohletz KH (1983) Hydrovolcanism: basic considerations and review. J Volcanol Geotherm Res 17:1–29

Sundararaj U, Macosko CW (1995) Drop breakup and coalescence in polymer blends: the effects of concentration and compatibilization. Macromolecules 28:2647–2657

Trigila R (2004) Laboratory experiments on magma-water interaction: vesiculating melt and explosive interaction. In: Abstracts of 32nd International Geological Conference, Florence (Italy), Aug 20–28, 2004

White JDL (1996) Impure coolants and interaction dynamics of phreatomagmatic eruptions. J Volcanol Geotherm Res 74:155–170

White JDL, Houghton B (2000) Surtseyan and related phreatomagmatic eruptions. In: Sigurdsson H et al (eds) Encyclopedia of volcanoes. Academic Press, San Diego, pp 495–512

Wohletz KH (1986) Explosive magma-water interactions: thermodynamics, explosion mechanisms, and field studies. Bull Volcanol 48:245–264

Wohletz KH, Heiken G (1992) Volcanology and geothermal energy. University of California Press, Berkeley, pp 1–432

Zimanowski B (1998) Phreatomagmatic explosions. In: Freundt A, Rosi M (eds) From magma to tephra, developments in volcanology 4. Elsevier, Amsterdam, pp 25–54

Zimanowski B, Büttner R (2002) Dynamic mingling of magma and liquefied sediments. J Volcanol Geotherm Res 114:37–44

Zimanowski B, Froehlich G, Lorentz V (1991) Quantitative experiments on phreatomagmatic explosions. J Volcanol Geotherm Res 48:341–358

Zimanowski B, Buttner R, Lorenz V (1997) Premixing of magma and water in MFCI experiments. Bull Volcanol 58:491–495

Zimanowski B, Büttner R, Koopmann A (2004) Experiments on magma mixing. Geophys Res Lett 31:L09612. DOI: 10.1029/2004GL019687